

Yersinia Virulence Depends on Mimicry of Host Rho-Family Nucleotide Dissociation Inhibitors

Gerd Prehna,¹ Maya I. Ivanov,² James B. Bliska,² and C. Erec Stebbins^{1,*}

¹Laboratory of Structural Microbiology, Rockefeller University, New York, NY 10021, USA

²Department of Molecular Genetics and Microbiology and Center for Infectious Diseases, Stony Brook University, Stony Brook, NY 11794, USA

*Contact: stebbins@rockefeller.edu

DOI 10.1016/j.cell.2006.06.056

SUMMARY

Yersinia spp. cause gastroenteritis and the plague, representing historically devastating pathogens that are currently an important bio-defense and antibiotic resistance concern. A critical virulence determinant is the *Yersinia* protein kinase A, or YpkA, a multidomain protein that disrupts the eukaryotic actin cytoskeleton. Here we solve the crystal structure of a YpkA-Rac1 complex and find that YpkA possesses a Rac1 binding domain that mimics host guanine nucleotide dissociation inhibitors (GDIs) of the Rho GTPases. YpkA inhibits nucleotide exchange in Rac1 and RhoA, and mutations that disrupt the YpkA-GTPase interface abolish this activity in vitro and impair in vivo YpkA-induced cytoskeletal disruption. In cell culture experiments, the kinase and the GDI domains of YpkA act synergistically to promote cytoskeletal disruption, and a *Y. pseudotuberculosis* mutant lacking YpkA GDI activity shows attenuated virulence in a mouse infection assay. We conclude that virulence in *Yersinia* depends strongly upon mimicry of host GDI proteins by YpkA.

INTRODUCTION

Nearly 200 million people are estimated to have died in the plague epidemics that devastated the ancient world (Perry and Fetherston, 1997), and the successful weaponization of plague in the former Soviet Union bioweapons program has made this pathogen a primary bio-defense concern (Henderson, 1999; Inglesby et al., 2000). Additional medical concerns arise from the evolution of multidrug resistant strains of the plague bacterium that have been reported in several locations from patient isolates (Galimand et al., 1997; McCormick, 1998). The plague is caused by the bacterial pathogen *Yersinia pestis*, which,

along with the food-borne agents of gastroenteritis, *Y. enterocolitica*, and *Y. pseudotuberculosis*, shares the highly conserved *Yersinia* virulence plasmid, or pYV, which is necessary to cause disease (Cornelis et al., 1998). This plasmid harbors numerous genes, a large number of which are associated with a type III protein secretion system (T3SS) that confers the ability of diverse pathogens to deliver virulence factors into host cells (Galán and Collmer, 1999). The translocated virulence factors of *Yersinia* include a protein tyrosine phosphatase, a cysteine protease, and a GTPase-activating protein, among others, and collaborate to disrupt and impair the normal cytoskeletal regulation in macrophages and polymorphonuclear neutrophils (PMNs) to achieve an antiphagocytic effect (Viboud and Bliska, 2005; Aepfelbacher et al., 1999; Aepfelbacher, 2004; Cornelis, 2000, 2002).

An important virulence factor of *Yersinia* spp. is the *Yersinia* protein kinase A, or YpkA (also called YopO in *Y. enterocolitica*), a substrate of the T3SS, which was first identified through its important contribution to disease progression and a region of sequence homology to eukaryotic serine/threonine kinases (Galyov et al., 1993). *Y. pseudotuberculosis* mutants with disruptions in YpkA have shown severely attenuated virulence in mouse infection models (Galyov et al., 1993, 1994). YpkA is an 82 kDa multidomain protein, which, in addition to the protein kinase, possesses a domain that binds to the small GTPases RhoA and Rac1, a domain required for activation by actin, and a relatively uncharacterized N-terminal domain (Barz et al., 2000; Dukuzumuremyi et al., 2000; Galyov et al., 1993, 1994; Hakansson et al., 1996; Juris et al., 2000).

In cultured cells, YpkA appears to function primarily in disrupting the host actin cytoskeleton (Dukuzumuremyi et al., 2000; Häkansson et al., 1996; Juris et al., 2000). Cells transfected with YpkA, or exposed to strains of *Yersinia* preferentially translocating YpkA over other virulence factors, lose their actin stress fibers and tend to round up and detach upon prolonged exposure (Häkansson et al., 1996; Juris et al., 2000; Nejedlik et al., 2004). Interestingly, this effect appears to be only partially associated with the kinase activity, as mutations in the active site attenuate,

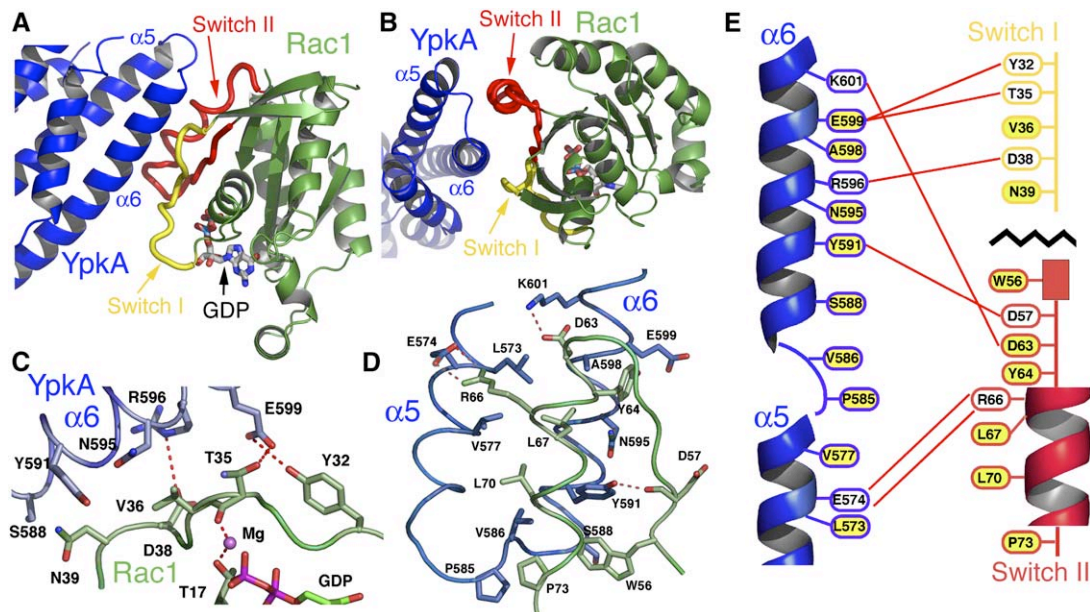


Figure 2. The YpkA-Rac1 Interface

(A) Ribbon diagram view of the Contact A interaction between YpkA and Rac1. Switch I (yellow) and Switch II (red) are highlighted, and GDP is noted. (B) The image in panel (A) rotated by 90° about a horizontal axis. (C) Close up of the Switch I interactions with the $\alpha 6$ helix of YpkA. Hydrogen bonds are denoted by dashed red lines. (D) Close up of the Switch II interactions with the $\alpha 5$ and $\alpha 6$ helices of YpkA. Hydrogen bonds are denoted by dashed red lines. (E) Schematic of the interactions of the $\alpha 5$ and $\alpha 6$ helices of YpkA with Switch I and Switch II of Rac1. Hydrogen bonds are indicated by red lines between the interacting residues, and hydrophobic interactions are shown with a yellow background.

and (4) a heterodimer appears to be the biological unit as judged by biochemical experiments (Figures 3 and S2).

The overall structure of YpkA (434–732) reveals an elongated, all-helical molecule consisting of two distinct subdomains connected by a 65 Å long “backbone” or “linker helix” (Figures 1A and 1B). The N-terminal subdomain contains most of the sequence-identified, ACC finger-like repeats that resemble, at the sequence level, elements required in host factors for small GTPase binding, whereas the C-terminal subdomain contains the sequence implicated in actin activation. The overall surface of the molecule is highly charged, containing a large basic patch in the GTPase binding domain and a large acidic patch in the actin-activation domain (Figure S3).

Despite apparent sequence similarities, the N-terminal subdomain of YpkA (residues 434–615) does not share the coiled-coil fold of host ACC fingers, but instead it consists of six helices organized into two three-helix bundles packed against each other. Each of the bundles is stabilized by hydrophobic zipping in the core, and extensive hydrophobic packing is observed between the bundles. The previously identified regions harboring sequence similarity with ACC fingers (Dukuzumuremyi et al., 2000; Maesaki et al., 1999a, 1999b) are not involved in the YpkA-Rac1 interface. The far C-terminal subdomain of YpkA, containing the polypeptide implicated in actin activation (residues 705–732, corresponding to helix $\alpha 10$), is a novel and elongated fold consisting of four helices clus-

tered into two pairs that only moderately interact with each other. The $\alpha 10$ helix (residues 705–730) encompasses the peptide that had been predicted to play a role in the interaction of YpkA with actin, and past work has shown that the deletion of the region eliminates both the ability of YpkA to bind to actin and kinase activity (Juris et al., 2000). This helix forms an integral part of the fold of this subdomain, contributing a large number of nonpolar residues to its hydrophobic core.

There are very few conformational changes between YpkA (434–732) crystallized alone and YpkA (434–732) in complex with Rac1 (Figure S3). Most differences are located in the C-terminal subdomain of YpkA and involve a slight overall displacement in the positioning of the $\alpha 7$ and $\alpha 8$ helices, as well as alterations in the conformation and relative disorder of solvent exposed loops. Rac1 is little altered by the binding of YpkA except for in the Switch regions as discussed below.

The YpkA-Rac1 Interface

YpkA and Rac1 form an interface burying roughly 1600 Å² and limited to residues 573–601 of YpkA (spanning the helices $\alpha 5$ and $\alpha 6$) contacting the key regulatory Switch I and Switch II regions of Rac1 (Figures 2A–2E). Switch I and Switch II together create a concave pocket into which the $\alpha 6$ (backbone) helix of YpkA inserts (Figure 2B), which, along with the clustering of the Switch II helix with the $\alpha 5$ and $\alpha 6$ helices, cement the interaction tightly.

The Switch I contacts involve a large number of hydrophobic, van der Waals interactions with YpkA, as well as several hydrogen bonds at this surface (e.g., residues Asp38 [Rac1] and Arg596 [YpkA], Glu599 [YpkA] and Tyr32 and Thr35 of Rac1; [Figures 2C and 2E](#)). A striking aspect of this interaction with Switch I is that YpkA contacts the conserved Thr35 residue, which is normally involved in magnesium ion coordination ([Dvorsky and Ahmadian, 2004](#)), resulting in a stable coordination network between the side chain of YpkA Glu599, Rac1 Tyr32, the hydroxyl group of Thr35, its main chain carbonyl oxygen, the magnesium ion, and the hydroxyl group of Thr17 ([Figure 2C](#)).

At Switch II, the molecular interface between YpkA and Rac1 is quite extensive, forming the largest portion of the protein-protein interactions ([Figures 2A, 2B, 2D, and 2E](#)). Most of the contacting residues between YpkA and Rac1 are involved in hydrophobic, van der Waals interactions forming a nonpolar interface between the $\alpha 5$ and $\alpha 6$ helices of YpkA and the α helix and surrounding loops of Switch II. Residues Leu573, Val577, and Val586 of YpkA, along with Leu67 and Leu70 of Rac1, contribute significantly to this hydrophobic interface, making what resembles a hydrophobic zipper motif between the $\alpha 5$ and $\alpha 6$ helices of YpkA and the helical element of Switch II ([Figures 2A, 2B, and 2D](#)). This interface between the molecules also includes YpkA Pro585 contacting Rac1 Pro73 at one end, “pinching” off the zipper, along with Tyr591, Asn595, and Ala598 (YpkA) and Trp56 and Asp63 (Rac1), making several van der Waals contacts between each other and the hydrophobic zipper motif. Additionally, Rac1 Tyr64 makes van der Waals contacts with YpkA Glu599, possibly helping to position it for the hydrogen bonding interactions to Tyr32 and Thr35 in the Switch I region of Rac1 described above. Although the binding surface is primarily hydrophobic in nature, it is also stabilized by three polar interactions. The main chain carbonyl oxygen of Rac1 Asp57 forms a hydrogen bond with the phenol group hydroxyl of YpkA Tyr591, as does the acidic group of Rac1 Asp63 with the amino group of YpkA Lys601. Finally, a salt bridge is formed between Rac1 Arg66 and YpkA Asp574 ([Figure 2D](#)).

To examine the importance of these contacts to complex stability, we mutated three residues of YpkA at the Contact A interaction surface and tested the purified protein for binding to Rac1 and RhoA. The triple mutant consisted of loss-of-contact mutations to alanine (Tyr591Ala, Asn595Ala, and Glu599Ala). Although these mutations do not destabilize YpkA itself, they completely abolish complex formation with both Rac1 and RhoA ([Figure 3](#)), strongly supporting the crystallographic analysis. In contrast, mutations in the second binding site in the crystals (Contact B, [Figure 1A](#)) had no effect on complex formation ([Figure 3](#)).

YpkA Mimics Host GDI Proteins

A comparison of the *Yersinia* YpkA interaction with Rac1 reveals intriguing similarities to the complexes between

host cell GDIs and their target Rho family GTPases. An alignment of the complexes of RhoGDI-1(α)-Rac1 ([Grizot et al., 2001](#)) and RhoGDI-2(LyGDI)-Rac2 ([Scheffzek et al., 2000](#)) with YpkA-Rac1 reveals that the Switch I polypeptide adopts a very similar conformation in all of these structures ([Figure 4A](#)). In addition, the residues of Switch I that make contacts with the host cell GDIs possess nearly identical conformations in the Rac1 complex with YpkA ([Figure 4C](#)). YpkA even appears to mimic a hallmark of the RhoGDI-small GTPase interaction by using an acidic residue to contact Thr35 of the small GTPase to form a highly stable coordination network involving YpkA Glu599, the hydroxyl group of Thr35, the carbonyl oxygen of Thr35 with the magnesium ion, and the hydroxyl oxygen of Thr17 ([Grizot et al., 2001](#); [Scheffzek et al., 2000](#)). This structural stabilization of Switch I in the GDP bound conformation results in an inhibition of nucleotide exchange. YpkA, therefore, possesses the key contacts seen between host RhoGDIs and their target GTPases at Switch I ([Figures 4A and 4C](#)).

YpkA contacts many of the same residues in Switch II as RhoGDI, although the details of the molecular interactions differ ([Figure 4C](#)). For example, the conformation of Switch II in the YpkA Rac1 structure is different from that seen in RhoGDI complexes with small GTPases, where Switch II is found in a conformation nearly identical to the GTP bound forms of the small G proteins. YpkA instead contacts these residues in Switch II in such a manner as to stabilize the region in a conformation similar to the structures of the GTPases bound to GDP. Indeed, both Switch I and Switch II of Rac1 in the YpkA structure are almost identical to the crystal structure of RhoA bound to GDP ([Wei et al., 1997](#)), indicating that YpkA acts to lock the small GTPase in the GDP bound, or physiologically “off,” conformation. RhoGDIs are so named for their ability to maintain small GTPases in an “inactive” physiological state, specifically through the inhibition of nucleotide exchange in the small GTPases. This inhibition is achieved by stabilizing the coordination of the magnesium ion and preventing both the ion and the bound GDP/GTP from dissociating ([Scheffzek et al., 2000](#)). This prevents both intrinsic exchange of the GDP/GTP nucleotide and that catalyzed by guanidine nucleotide exchange factors, or GEFs.

Given the similarities at the structural level with host RhoGDIs, we therefore examined whether YpkA could inhibit the intrinsic and catalyzed exchange of nucleotides for Rac1, RhoA, and Cdc42. As shown in [Figure 5A](#), when Rac1, RhoA, or Cdc42 are incubated in the presence of mant-GTP, a fluorescent nucleotide analog, there is an increase of fluorescence signal over time, indicating that increasing amounts of the labeled nucleotide have been bound ([Experimental Procedures](#)). The addition of YpkA (434–732) results in a marked decrease in nucleotide exchange for Rac1 and RhoA, but only a modest decrease for Cdc42 ([Figure 5A](#)). In contrast, the triple mutant (Contact A mutant) of YpkA that is impaired in Rac1 and RhoA binding was unable to inhibit the exchange of GTP ([Figure 5A](#)). Similar results are observed if we challenge

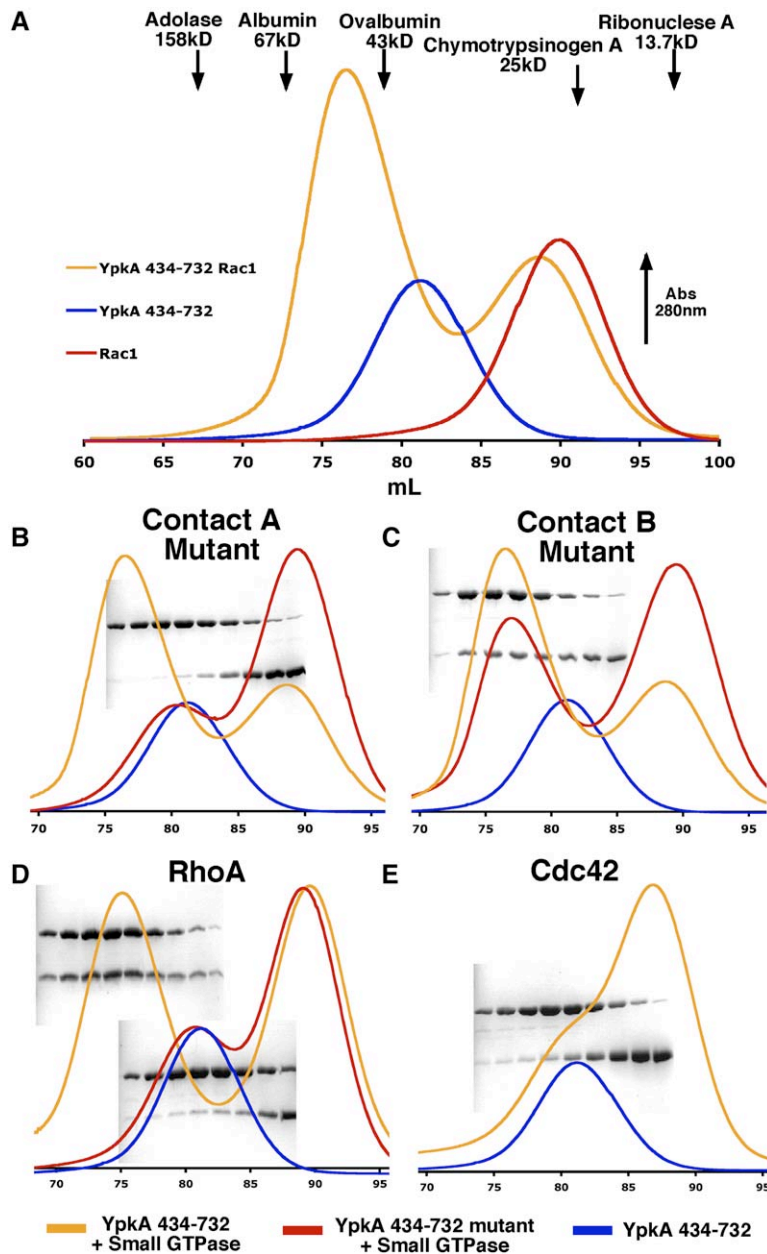


Figure 3. Gel Filtration and Mutagenesis

(A) The gel filtration profile of YpkA (434–732). The molecular weight standards used in the column calibration are labeled above the graph with the arrows indicating their approximate elution volume. YpkA (434–732) is shown in blue, Rac1 is shown in red, and the YpkA (434–732) and Rac1 complex is shown in orange.

(B) The gel filtration profile of the YpkA (434–732) Contact A mutant. YpkA (434–732) Contact A mutant in the presence of Rac1 is shown in red, the YpkA (434–732) and Rac1 complex is shown in orange, and the elution peak of YpkA (434–732) is shown in blue. The gel of fractions containing the eluted material is overlain on the graph.

(C) The gel filtration profile of the YpkA (434–732) Contact B mutant. YpkA (434–732) Contact B mutant in the presence of Rac1 is shown in red, the YpkA (434–732) and Rac1 complex is shown in orange, and the elution peak of YpkA (434–732) is shown in blue.

(D) The gel filtration profile of the YpkA (434–732) interaction with RhoA. YpkA (434–732) in the presence of RhoA is shown in orange, the YpkA (434–732) Contact A mutant and RhoA complex is shown in red, and the elution peak of YpkA (434–732) is shown in blue. SDS-PAGE analysis (stained with Coomassie blue) of fractions containing the material from YpkA (434–732) and the YpkA (434–732) Contact A mutant with RhoA are superimposed on the corresponding chromatograms.

(E) The gel filtration profile of the YpkA (434–732) interaction with Cdc42. YpkA (434–732) in the presence of Cdc42 is shown in orange and the elution peak of YpkA (434–732) is shown in blue. SDS-PAGE analysis (stained with Coomassie blue) of fractions containing the material from YpkA (434–732) and Cdc42 is superimposed on the chromatogram.

the system with a potent GEF, *Salmonella* SopE (Buchwald et al., 2002; Friebe and Hardt, 2000; Hardt et al., 1998; Rudolph et al., 1999). SopE, one of the most active exchange factors studied to date (Friebe and Hardt, 2000; Rudolph et al., 1999), quickly catalyzed the exchange of the bound GDP of Rac1, RhoA, and Cdc42 with the mant-GTP (Figure 5B). Incubation of Rac1 or RhoA with increasing amounts of YpkA leads to a dose-dependent decrease in exchange when challenged by SopE (Figure 5B). In contrast, YpkA was unable to inhibit exchange in Cdc42 catalyzed by SopE (Figure 5C). As was observed with the intrinsic nucleotide exchange of Rac1 and RhoA, the triple mutant of YpkA was completely inactive against

SopE. We therefore conclude that the YpkA C-terminal domain is a potent inhibitor of nucleotide exchange for Rac1 and RhoA in vitro.

We then sought to establish the in vivo significance of binding to RhoA and Rac1, and thereby, presumably, the biological significance of the GDI-like activity of YpkA. To address this, we transfected cultured human intestinal epithelial cells (Henle407) with the following six YpkA constructs: 1–732 (wild-type), 1–732 (K272A, kinase active site mutant), 1–732 (Contact A mutant), 1–732 (K272A + Contact A mutant), 434–732, and 434–732 Contact A mutant (Experimental Procedures). After 24 hr the cells were immunostained for the YpkA constructs with

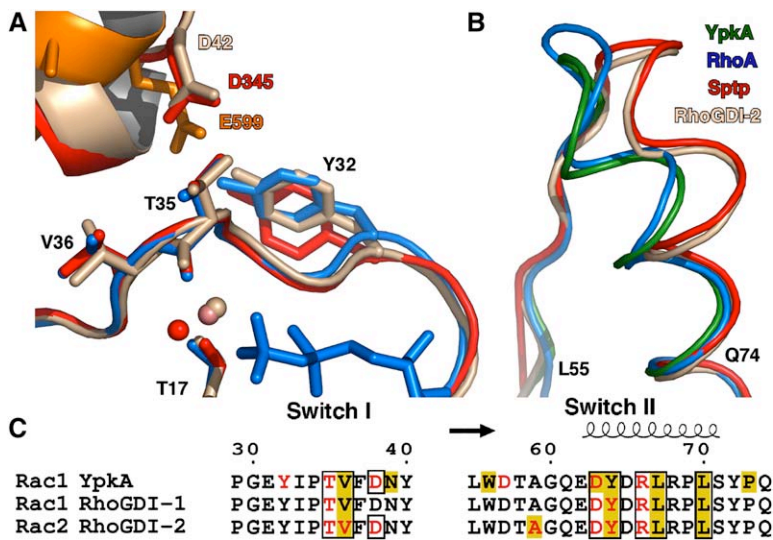


Figure 4. YpkA Mimics the Binding of Host Cell GDIs

(A) Structural alignment between YpkA-Rac1 with the RhoGDI-1(α)-Rac1 and the RhoGDI-2 (LyGDI)-Rac2 complexes at Switch I. YpkA is indicated in orange, Rac1 bound to YpkA is indicated in blue, the RhoGDI-1(α) Rac1 structure in red and the RhoGDI-2(LyGDI) Rac2 structure in tan. The GDP molecule from the YpkA-Rac1 complex structure is shown in blue.

(B) Structural alignment between the YpkA-Rac1, RhoAGDP, SptP-Rac1, and RhoGDI-2 (LyGDI)-Rac2 complexes at Switch II. The YpkA complex is indicated in green, the RhoA-GDP structure in blue, the SptP-Rac1-GDP-AlF₃ complex in red, and the RhoGDI-2 (LyGDI)-Rac2 complex in tan. The residues at the N and C terminus of the region in Rac1 shown are labeled.

(C) The conserved interactions of YpkA and GDI proteins with Rho family GTPases is

shown. Both Switch I and Switch II are indicated with the secondary structural elements of the YpkA-Rac1 structure drawn above. Residues involved in hydrogen bonding are drawn in red, and those residues making hydrophobic or Van der Waals contacts are highlighted in yellow. Similar interactions between YpkA and the RhoGDI proteins are boxed.

antibodies against an N-terminal FLAG epitope ([Experimental Procedures](#)) and the cytoskeleton visualized by staining with Rhodamine Phalloidin. As has been reported ([Håkansson et al., 1996](#); [Juris et al., 2000](#); [Nejedlik et al., 2004](#)), transfection with wild-type YpkA induces extensive cytoskeletal disruption, leading to a loss of actin stress fibers and a distortion in the cellular morphology. In fact, transfection of YpkA into mammalian cells induces two observable effects, the first causing the disappearance of actin stress fibers and the second resulting in severe cellular deformation in addition to the loss of stress fiber formation ([Figure 6](#)). This cellular deformation has been described as a “rounding up” of the cells but maintaining focal adhesions ([Juris et al., 2000](#)). Full-length YpkA shows the ability to both prevent stress fiber formation and causes a large number of the Henle cells to lose their shape, resulting in the described cellular deformation or “wild-type” effect ([Figure 6B](#)). Transfection with the N-terminal deletion construct YpkA (434–732), which lacks the serine-threonine kinase domain, results in an attenuated or “intermediate” phenotype. YpkA (434–732) is able to cause the disappearance of actin stress fibers in most cells, although its ability to cause cellular deformation is reduced as compared to the wild-type construct ([Figure 6A](#)). The YpkA (434–732) Contact A mutant, which is deficient for both Rac1 and RhoA binding, in addition to GDP dissociation inhibition *in vitro*, leads to a complete loss of cytoskeletal disruption ([Figure 6B](#)).

In the context of the full-length protein, these same mutations are intriguing. To begin, YpkA with the kinase active site mutation K272A is only slightly attenuated in cytoskeletal disruption, losing most of the wild-type effect but maintaining a significant amount of the intermediate effect ([Figure 6A](#)). In fact, this mutant is nearly identical in its effect on cells to the deletion of the entire kinase domain. In

contrast, the YpkA Contact A mutant, defective for binding to Rac1 and RhoA (and defective for GDI-like activity) causes a very low level of cytoskeletal alterations, and adding to this mutant, the K272A kinase mutation does not appreciably change the phenotype. Although the full-length YpkA Contact A mutant and the K272A Contact A mutant do not cause significant cytoskeletal alterations, they are observed to localize to the membrane ([Figure 6B](#), data not shown). As both the 434–732 construct and the 434–732 Contact A mutant are seen uniformly distributed throughout the cell, this supports the previously reported results that membrane localization is not dependent upon small GTPase binding and may be dependent upon a signal in the N terminus of YpkA ([Dukuzumuremyi et al., 2000](#)).

Altogether, these results strongly suggest that the C-terminal, GDI-like activity of YpkA is the more significant contributor to cytoskeletal effects. The kinase domain does appear to work synergistically with the GDI-like domain, however, as evinced in both the reduced wild-type effect of the kinase active site mutant as well as the complete loss of activity in the YpkA (434–732) GDI (Contact A) mutant. Interestingly, the double mutant of kinase and GDI does not completely abolish cytoskeletal effects, perhaps due to residual kinase activity present in the K272A mutation ([Dukuzumuremyi et al., 2000](#); [Juris et al., 2000](#)).

In order to establish the relevance of these biochemical and cell biological data to infection, we examined the virulence phenotypes of *Y. pseudotuberculosis* *ypkA* mutants in a mouse infection assay. Two such mutants were tested, a *ypkA* null mutant, in which the entire *ypkA* reading frame was deleted, and a *ypkA* Contact A mutant, in which the Tyr591Ala, Asn595Ala, and Glu599Ala codon substitutions were introduced onto the virulence plasmid. Analysis by SDS-PAGE of the Yops secreted by these

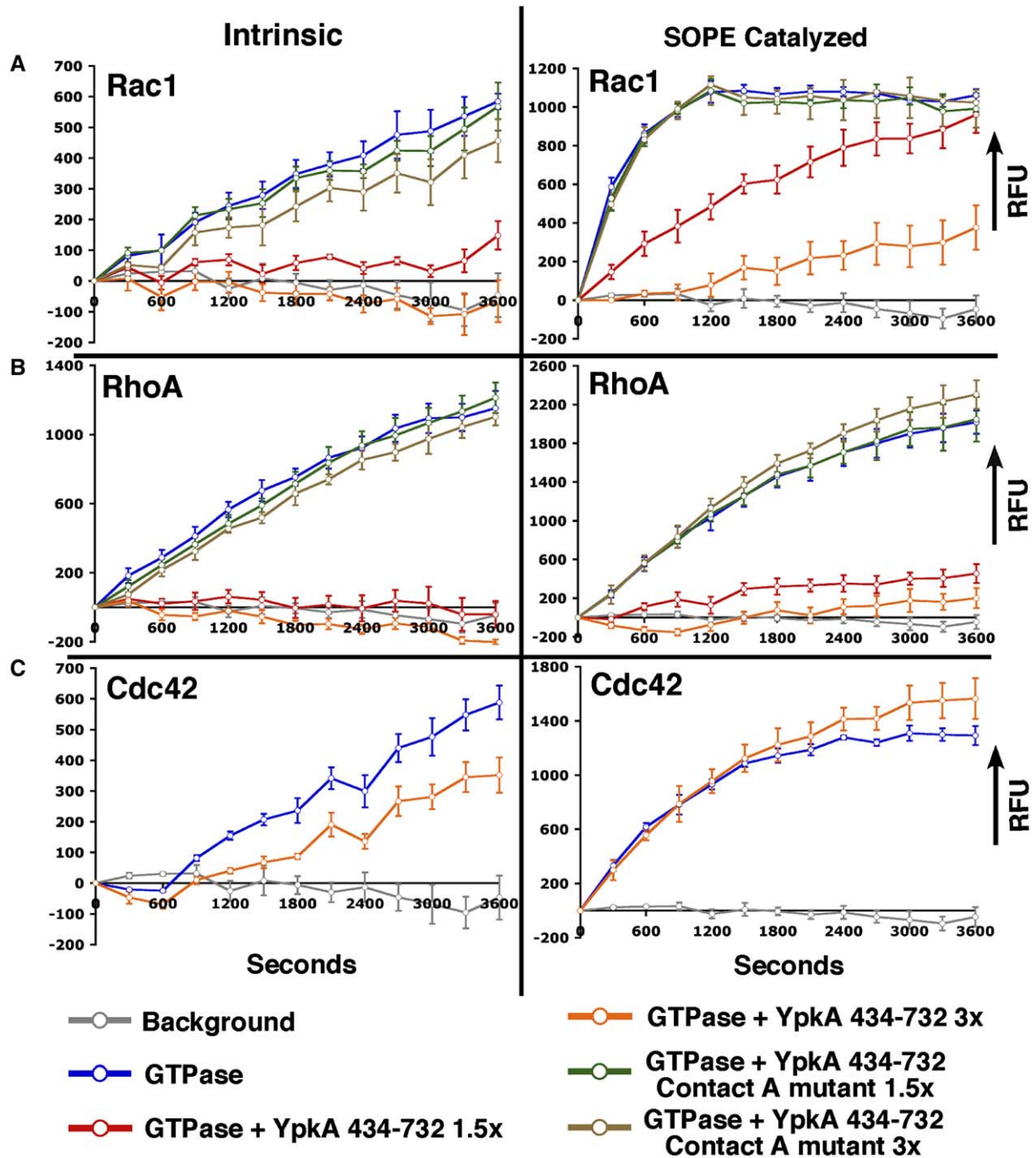


Figure 5. YpkA Inhibits Nucleotide Exchange in Rac1 and RhoA

The intrinsic and GEF catalyzed rate of mant-GTP exchange into the small GTPases Rac1, RhoA, and Cdc42 was monitored as described in [Experimental Procedures](#). The left column shows the intrinsic rate inhibition data, and the right column shows the rate inhibition data when challenged with the *Salmonella* GEF SopE. Panel (A) is Rac1, panel (B) is RhoA, and panel (C) is Cdc42. The experiments are shown with the increase of relative fluorescence units (RFU) over time in seconds. The labels are described in a legend below the figure, where 1.5 \times and 3 \times are relative molar concentrations of YpkA or YpkA Contact A mutant above the small GTPase. Error bars (panels A-C) represent the standard deviation (from the mean value plotted) calculated from a minimum of three independent experiments.

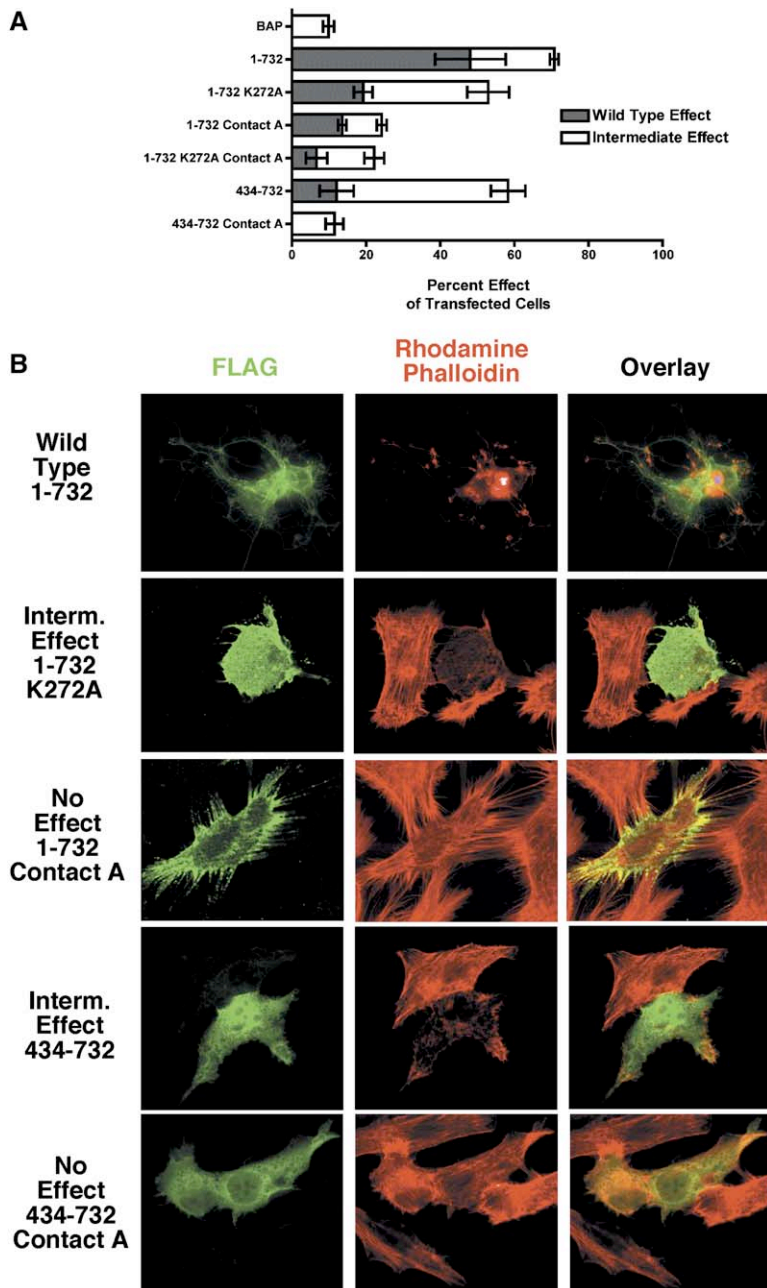


Figure 6. GDI Activity Is Critical for YpkA to Promote Cytoskeletal Alterations

(A) The bar graph represents the percentage of transfected cells with cytoskeletal alterations and the contribution of the observed wild-type phenotype and the observed intermediate phenotype to the total percentage. The wild-type phenotype is indicated in gray and the intermediate phenotype in white. Bacterial Alkaline Phosphatase, BAP, is the negative control; 1-732 is wild-type YpkA; 1-732 K272A is a kinase inactive mutant of YpkA; 1-732 Contact A is YpkA with the Contact A mutant; 1-732 K272A Contact A is the kinase inactive mutant plus the Contact A mutant; 434-732 is the crystallized construct; 434-732 Contact A is the Contact A mutant (RhoA/Rac1 binding deficient structure-based mutant). Error bars (panels A-C) represent the standard deviation (from the mean value plotted) calculated from a minimum of three independent experiments. (B) Examples of the visualization of YpkA by the immunostaining of transfected HeLa407 cells. Each of the three observed phenotypes is shown with staining for both the epitope, FLAG-tagged YpkA and for the actin cytoskeleton (Experimental Procedures). Each row is labeled by the construct transfected. The first column shows the presence of expression of the FLAG-tagged YpkA constructs and is colored in green. The second column shows the immunostaining of the actin cytoskeleton by rhodamine phalloidin in red, and the last column is the overlay of the fluorescent signals.

strains showed that the null mutant did not secrete YpkA protein, while the Contact A mutant secreted a full-length polypeptide (Figure S5A). Immunoblot analysis of secreted Yops showed that YopT and YopE were secreted at native levels by the null mutant and Contact A mutant (Figures S5B and S5C). In addition, the results of a HeLa cell rounding assay indicated that the null mutant and Contact A mutant translocated YopT and YopE into host cells at normal levels (Figure S6). Mice were infected intragastrically with one of the mutants, or the isogenic parental strain, and the animals were monitored for survival over a 14 day period. As shown in Figure 7, all eight

mice infected with the wild-type strain succumbed to the infection by day 9, while only two mice infected with the Contact A mutant died, one on day 7 and one on day 12. The survival curves for the mice infected with the wild-type or Contact A mutant strains were significantly different ($P = 0.0003$), as determined by a logrank test. Interestingly, all mice infected with the *ypkA* null mutant died by day 8 (Figure 7), a survival rate not significantly different from the wild-type control ($P = 0.7333$). Other groups studying pathogenesis of *Yersinia ypkA* null mutants in mouse infection assays have recently reported similar findings, in that strains lacking the *ypkA* gene appear to

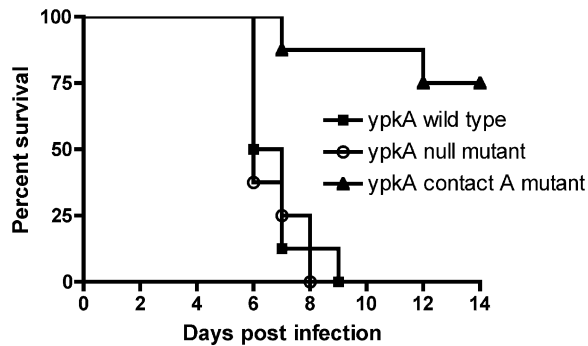


Figure 7. The GDI Activity of YpkA Is Critical for *Yersinia* Virulence

Groups of mice were infected intragastrically with 5×10^9 CFU of wild-type *Y. pseudotuberculosis*, a *ypkA* null mutant, or a *ypkA* Contact A mutant. Survival of the mice was recorded over a 14 day period. Results shown are compiled from two independent experiments that were performed with groups of four mice (logrank value of $P = 0.0003$ between the wild-type and Contact A mutant curves).

be as virulent as parental strains (Logsdon and Mecsas, 2003; Trülsch et al., 2004). In contrast, *Y. pseudotuberculosis* strains that express the altered YpkA protein lacking the GDI activity are clearly attenuated for virulence (Figure 7). Taken together, these findings indicate that the GDI activity of YpkA is critical for *Yersinia* virulence.

DISCUSSION

A Host GDI Mimic Crucial to Virulence in *Yersinia*

Virulence in *Yersinia pseudotuberculosis* depends upon the translocated virulence factor YpkA (Galyov et al., 1993), a protein that is very highly conserved in the plague pathogen, *Yersinia pestis*. Despite the known importance to virulence, little has been forthcoming in understanding the mechanism of activity of YpkA. This has been particularly true of the C-terminal domain of the protein, which, while known to bind Rho GTPases, has remained enigmatic in terms of function.

The cocrystal structure of a C-terminal domain of YpkA and Rac1 reveals that this bacterial virulence factor is a mimic of host Rho-family GDI proteins in its binding to the GTPase and also in its ability to inhibit nucleotide exchange. Loss-of-contact mutations in YpkA that impair Rac1 and RhoA binding abolish this GDI-like activity, and severely diminish the cytoskeletal disruption induced by this domain. Furthermore, these mutations severely decrease *Yersinia* virulence in a mouse model of infection. Altogether, these data strongly suggest that YpkA mimics host GDI proteins by acting as an “off switch” to modulate the Rac1-associated signaling pathways that regulate host cytoskeletal structure.

Collaborative Inactivation of Small GTPases by *Yersinia* Outer Proteins

Interestingly, despite the fact that YpkA mimics key aspects of GDI function, it does not possess all the activities

of its host cell counterparts. Host cell RhoGDIs are also able to slow the intrinsic rate of GTP hydrolysis by small GTPases and, more importantly, have a specialized domain that the protein uses to bind the isoprenylated tail of small GTPases to remove them from the cell membrane. Although YpkA can bind to both the GDP and GTP conformations of RhoA and Rac1 (Dukuzumuremyi et al., 2000) and inhibit nucleotide release, it only has a moderate effect on the intrinsic rate of GTP hydrolysis (data not shown). Moreover, YpkA does not possess any clear analog of the β sheet motif necessary to bind an isoprenyl group, and it seems likely that YpkA has no such function. This may in fact be reasonable, as another *Yersinia* virulence factor that is translocated into host cells along with YpkA, YopT, removes any selective pressure for such a membrane removing GDI-like activity. This is because YopT, a cysteine protease that specifically cleaves off the C-terminal tail residues of the RhoGTPases Cdc42, Rac1, and RhoA, removes the small GTPases from the membrane in a highly efficient manner (Shao et al., 2002). Moreover, *Yersinia* also translocates into host cells YopE, a GAP or GTPase activating protein essential for virulence, that quickly catalyzes the hydrolysis of GTP bound to small GTPases of the Rho family (Black and Bliska, 2000). Therefore, between YpkA and YopT, two of the physiological effects of a RhoGDI can be recapitulated. The final activity seen in many host RhoGDIs, the inhibition of GAP activity on the RhoGTPases, would be counterproductive and interfere with the function of YopE. Thus, YpkA appears to be perfectly engineered to work in concert with YopE and YopT.

Synergy between Kinase and GDI Domains

Our data suggest an explanation of previous results obtained in the work by Juris et al., 2000. In their research, HeLa cells were transfected with vectors expressing wild-type YpkA, a YpkA kinase inactivated mutant (K269A of *Yersinia enterocolitica* YopO, equivalent to K272A of *Yersinia pseudotuberculosis* YpkA), and a C-terminal deletion construct that prevented kinase activity, reporting that, compared to the wild-type phenotype, the kinase inactive mutant exhibited an intermediate phenotype where actin stress fiber formation was disrupted, but the actin microfilament system partially remained. This observation is consistent with our observations that YpkA (434–732) alone, as well as full-length YpkA K272A, are sufficient to disrupt stress fiber formation as well as to cause a low level of cellular deformation. Results with the C-terminal deletion constructs show that no cytoskeletal disruption activity is observed, although they contain the elements necessary for Rac1/RhoA binding. Our biochemical and structural results suggest that this may be explained by the aggregated and misfolded nature of these constructs (Figure S1) and not simply a lack of binding to actin. Taking into account our observations and the work by Juris et al., 2000, it is apparent that the full effect of YpkA function is achieved by both the kinase activity and the GDI activity of the C-terminal domain, although

our point mutants in cell culture argue that the GDI-like activity is the greater contributor.

Virulence Phenotypes of *ypkA* Mutants

In the initial work that reported the identification of YpkA, Galyov et al., 1993 demonstrated that two different *Y. pseudotuberculosis* *ypkA* mutants were attenuated for virulence in a mouse infection model. One attenuated mutant resulted from an in-frame deletion of *ypkA* codons 207–388, which removed a major portion of the kinase domain and produced a protein that was secreted by the T3SS but lacked kinase activity (Galyov et al., 1993). The other mutant produced a protein truncated after residue 548 that was also competent for secretion by the T3SS (Galyov et al., 1993). Taken at face value, these results suggested that both the kinase activity and a C-terminal region of YpkA were important for *Yersinia* virulence. However, it remained unclear how the C-terminal region of YpkA contributed to *Yersinia* virulence. Moreover, in recent studies, little or no role for YpkA in virulence could be found when *Yersinia* mutants containing a larger in-frame deletion of *ypkA* (codons 21–712) (Logsdon and Meccas, 2003), or a complete deletion of the *yopO* reading frame (Trülzsch et al., 2004), were utilized in mouse infection assays. By constructing a *Y. pseudotuberculosis* point mutant specifically defective for GDI function, we now demonstrate that this activity within the C-terminal domain of YpkA is critical for *Yersinia* virulence. We further confirmed the findings that mutations that remove most, or all, of the *ypkA* reading frame do not lead to attenuation of virulence in a mouse infection model (Logsdon and Meccas, 2003; Trülzsch et al., 2004). One possible explanation for these results is that null mutations in *ypkA* result in increased translocation of other Yop virulence factors in vivo, which compensates for the loss of YpkA function. If true, this type of phenomenon further underscores the power and importance of employing mutations that ablate the activity, and not the expression, of a suspected bacterial virulence determinant.

A Widespread Theme of Host Mimicry

It is becoming increasingly clear that a common strategy used by bacterial pathogens to modulate host cell biology is the mimicry of eukaryotic biochemical processes (Stebbins and Galán, 2001). This has been especially true of virulence factors that target the Rho GTPases in order to manipulate host cytoskeletal structure. We have presented data here that the *Yersinia* virulence factor YpkA, in addition to its host-like serine/threonine kinase activity, possesses an additional host mimicry by harboring key functions of the RhoGDI proteins, preventing nucleotide exchange in RhoA and Rac1 and thereby disrupting the host cytoskeleton. This fascinating interaction we show to exert a virulence effect, revealing another example of host mimicry in the virulence strategies of bacterial pathogens.

EXPERIMENTAL PROCEDURES

Cloning, Mutagenesis, and Protein Purification

The *Y. pseudotuberculosis* YpkA gene was cloned from the *Yersinia* virulence plasmid as an N-terminal fusion with glutathione-S-transferase (GST). To create the YpkA mutants, the amino acid substitutions were introduced by PCR using primers containing the appropriate base changes and subsequent removal of the template plasmid by digestion with Dpn I prior to transformation and verified by DNA sequencing. YpkA clones were transformed into BL21 (DE3) cells, and expression was induced with 1 mM IPTG for 16 hr at 20°C. YpkA constructs were affinity purified using a glutathione-sepharose resin, separated from GST by site-specific proteolytic cleavage and further purified by ion exchange and gel filtration chromatography.

Crystallography

YpkA (434–732) was reductively methylated following published protocols (Rypniewski et al., 1993) and crystallized at 4°C by hanging drop vapor diffusion using a 1:1 mixture of protein and well solution, which consisted of 100 mM CAPs pH 10.5, 140–180 mM NaCl, and 16% to 18% PEG1500. Rac1 was purified using a glutathione-sepharose resin, separated from GST by site-specific proteolytic cleavage, and further purified by ion exchange and gel filtration chromatography. The complex between methylated YpkA (434–732), and Rac1 1–184 bound to GDP was formed by first combining purified YpkA with an excess of Rac1 and then by isolation by gel filtration chromatography, and crystallized at 22°C by hanging drop-vapor diffusion using a 1:1 or 3:2 mixture of complex and well solution, which consisted of 100 mM HEPES pH 6.5–7.5, and 5% to 8% PEGMME2000. Phases for the monomer structure were determined using the anomalous signal from selenomethionine-substituted protein crystals using the SOLVE/RESOLVE package (Terwilliger, 2004). The partial model built by RESOLVE was then rebuilt and initially refined using ARP/wARP (Perrakis et al., 1999) with the native data set. The model generated by ARP/wARP was then refined using REFMAC5 (Murshudov et al., 1997) from the CCP4 suite of programs (CCP4, 1994; Potterton et al., 2003). The final model has an R/R_{free} of 20.9/23.8, with 96.4% of the residues in the most favored regions of the Ramchandran plot with no outliers. For the YpkA (434–732) and Rac1 1–184 GDP complex phases were determined by molecular replacement (search model 1MH1). The solution was then refined using REFMAC5 (Murshudov et al., 1997) from the CCP4 suite of programs (1994; Potterton et al., 2003; Winn et al., 2001, 2003). The final model has an R/R_{free} of 22.4/25.9.

Binding and Exchange Assays

The complex between YpkA (434–732) and Rac1 (1–184) was formed by first combining purified YpkA with an excess of Rac1, examining by gel filtration chromatography, and finally visualizing by SDS-PAGE. The Contact A mutant and Contact B mutant were purified as described for YpkA (434–732), and the complex with Rac1 was formed and analyzed as described for YpkA (434–732). Binding experiments with RhoA (F25N 1–181) and Cdc42 (1–184) were carried out in the same manner as Rac1. Both RhoA and Cdc42 were purified by GST affinity chromatography followed by gel filtration. Purified Rac1 or RhoA was incubated alone with buffer (20 mM Tris, pH 7.5, 50 mM NaCl, 5 mM MgCl₂) or with purified YpkA (434–732), YpkA (434–732) Contact A mutant for 10 min on ice. Both YpkA (434–732) and YpkA (434–732) Contact A mutant were added in either a 1.5-fold or in a 3-fold molar ratio access of Rac1. Purified Cdc42 was incubated alone with buffer or with purified YpkA (434–732) in a 3-fold molar ratio access. To initiate the intrinsic exchange reaction, the stock incubations were then added to reaction buffer (20 mM Tris, pH 7.5, 50 mM NaCl, 5 mM MgCl₂, and mant-GTP) resulting in a final concentration of Rac1 at 40 μM and mant-GTP at 100 μM. Reactions were then transferred to a 96-well plate and left for 5 min to bring to room temperature. The fluorescence of each reaction was measured every 5 min for a total

of 1 hr using a SpectraMax GeminiXS fluorimeter from Molecular Devices. An excitation wavelength of 355 nm and an emission wavelength of 448 nm with a cutoff of 435 nm was used to detect the presence of bound mant-GTP. SopE was added to each reaction after the 5 min incubation to room temperature at a final concentration of 0.22 μ M for Rac1 or RhoA and 0.04 μ M for Cdc42.

Transfections

YpkA constructs 1–732, 434–732, and 434–732 Contact A mutant (Tyr591A, Asn595A, Glu599A), were cloned into the pFLAG-CMV-4 mammalian expression vector using the restriction sites NotI and XbaI resulting in N-terminally tagged constructs. Henle407 cells were grown to confluence in DMEM media containing 10% Fetal Bovine Serum (FBS) and penicillin/streptomycin. The cells were then transferred to six-well tissue culture dishes containing a glass coverslip. Approximately 200,000 cells were added to each well with a total volume of 2 ml and grown overnight. The transfections were carried out using the Geneporter2 reagent and protocol (Genlantis). A total of 6 μ g of DNA was added to each reaction, and reactions were performed in triplicate. Reactions were allowed to proceed for 24 hr before being fixed and stained. Cells were fixed with 3% Formaldehyde, permeabilized with 0.5% Triton, and blocked with 3% BSA in PBS before exposure to antibodies. The YpkA constructs were visualized by primary antibody staining with mouse α -FLAG antibody (Sigma) and then by the secondary Alexa-Fluor goat α -mouse antibody (Molecular Probes). The actin cytoskeleton was visualized by staining with Rhodamine Phalloidin (Molecular Probes). To quantify the effect of each construct on the host cytoskeleton each reaction was counted blind and in triplicate. For each reaction, between 75 and 200 transfected cells were counted for each of the triplicate reactions (a total of 225–450 cells for each construct) and the state of their cytoskeleton scored as wild-type or intermediate effect. The cells were visualized by the use of an Axioplan2 upright microscope with Attoattic fluorescent filters and a Hamamatsu Digital Camera or by the use of a Zeiss LSM510 confocal microscope.

Yersinia Strains and Mouse Infection Assays

IP2777 is a virulent serogroup O1 strain of *Y. pseudotuberculosis* obtained from Michel Simonet (Simonet and Falkow, 1992). The LD50 of IP2777 in C57BL/6 mice challenged intragastrically is 5×10^8 CFU. YpkA null and Contact A mutants were constructed as described in the Supplemental Experimental Procedures. Two independent mouse infection experiments were carried out, and the results presented are compiled from the two experiments. Eight-week-old female C57BL/6 mice (Taconic) were challenged by the intragastric route using a 20 gauge feeding needle. Bacterial inocula were prepared from cultures grown in Luria Broth (LB) with shaking at 26°C. Bacteria were inoculated into LB, grown overnight, and subcultured in LB to an OD600 of 0.1. After a second overnight growth, the cultures were centrifuged, the bacterial pellets were washed once in Hank's balanced salt solution (HBSS), and suspended HBSS to yield 5×10^9 CFU per 0.2 ml. C57BL/6 mice were fasted for 18 hr prior to infection. Groups of four animals were infected with 0.2 ml of suspended bacteria (a dose equivalent to 10 LD50s). Infected mice were provided food and water and carefully observed three times a day over a 14 day period. Mice exhibiting severe signs of disease (ruffled fur, hunched posture, and immobility) were humanely euthanized by CO₂ inhalation. Survival curves were plotted using Prism (GraphPad) and analyzed for significant differences using the Mantel-Haenszel logrank test. These experiments were carried out in compliance with protocols approved by the IACUC at Stony Brook University.

Supplemental Data

Supplemental Data include six figures, two tables, and references and can be found with this article online at <http://www.cell.com/cgi/content/full/126/5/869/DC1/>.

ACKNOWLEDGMENTS

Protein N-terminal sequencing and mass-spectroscopic analysis were performed by the Protein Resource Center of the Rockefeller University under the direction of H. Deng. We thank H. Mueller at Rockefeller University, R. Udipi of Brookhaven beamline X9A, and W. Shi of Brookhaven Beamline X29 for access to and assistance with crystallographic equipment. We also thank Yue Zhang at Stony Brook University for help in developing conditions for the mouse infection assay and Lance Palmer at Stony Brook University for help with statistical analysis. This work was funded in part by research funds to C.E.S. from the Rockefeller University and PHS grants 1U19AI056510 (to C.E.S.) and RO1AI433890 (to J.B.B.) from the National Institute of Allergy and Infectious Diseases. Coordinates and structure factors have been deposited in the protein data bank under accession code 2H70 and 2H7V for the YpkA and YpkA-Rac1 structures, respectively. Protein biochemistry, structural biology, and cytoskeletal assays were performed by G.P. *Yersinia* strain constructions were performed by M.I.I. Mouse, and HeLa cell infections were performed by M.I.I. and J.B.B.

Received: November 9, 2005

Revised: April 20, 2006

Accepted: June 16, 2006

Published: September 7, 2006

REFERENCES

- Aepfelbacher, M. (2004). Modulation of Rho GTPases by type III secretion system translocated effectors of *Yersinia*. *Rev. Physiol. Biochem. Pharmacol.* 152, 65–77.
- Aepfelbacher, M., Zumbihl, R., Ruckdeschel, K., Jacobi, C.A., Barz, C., and Heesemann, J. (1999). The tranquilizing injection of *Yersinia* proteins: a pathogen's strategy to resist host defense. *Biol. Chem.* 380, 795–802.
- Barz, C., Abahji, T.N., Trülzsch, K., and Heesemann, J. (2000). The *Yersinia* Ser/Thr protein kinase YpkA/YopO directly interacts with the small GTPases RhoA and Rac-1. *FEBS Lett.* 482, 139–143.
- Black, D.S., and Bliska, J.B. (2000). The RhoGAP activity of the *Yersinia pseudotuberculosis* cytotoxin YopE is required for antiphagocytic function and virulence. *Mol. Microbiol.* 37, 515–527.
- Buchwald, G., Friebel, A., Galán, J.E., Hardt, W.D., Wittinghofer, A., and Scheffzek, K. (2002). Structural basis for the reversible activation of a Rho protein by the bacterial toxin SopE. *EMBO J.* 21, 3286–3295.
- CCP4 (Collaborative Computational Project, Number 4 (1994). The CCP4 suite: programs for protein crystallography. *Acta Crystallogr. D Biol. Crystallogr.* 50, 760–763.
- Cornelis, G.R. (2000). Molecular and cell biology aspects of plague. *Proc. Natl. Acad. Sci. USA* 97, 8778–8783.
- Cornelis, G.R. (2002). The *Yersinia* Ysc-Yop 'type III' weaponry. *Nat. Rev. Mol. Cell Biol.* 3, 742–752.
- Cornelis, G.R., Boland, A., Boyd, A.P., Geuijen, C., Iriarte, M., Neyt, C., Sory, M.P., and Stainier, I. (1998). The virulence plasmid of *Yersinia*, an antihost genome. *Microbiol. Mol. Biol. Rev.* 62, 1315–1352.
- Dukuzumuremyi, J.M., Rosqvist, R., Hallberg, B., Åkerström, B., Wolf-Watz, H., and Schesser, K. (2000). The *Yersinia* protein kinase A is a host factor inducible RhoA/Rac-binding virulence factor. *J. Biol. Chem.* 275, 35281–35290.
- Dvorsky, R., and Ahmadian, M.R. (2004). Always look on the bright side of Rho: structural implications for a conserved intermolecular interface. *EMBO Rep.* 5, 1130–1136.
- Friebel, A., and Hardt, W.D. (2000). Purification and biochemical activity of *Salmonella* exchange factor SopE. *Methods Enzymol.* 325, 82–91.

- Galán, J.E., and Collmer, A. (1999). Type III secretion machines: bacterial devices for protein delivery into host cells. *Science* 284, 1322–1328.
- Galimand, M., Guiyoule, A., Gerbaud, G., Rasoamanana, B., Chan-teau, S., Carniel, E., and Courvalin, P. (1997). Multidrug resistance in *Yersinia pestis* mediated by a transferable plasmid. *N. Engl. J. Med.* 337, 677–680.
- Galyov, E.E., Håkansson, S., Forsberg, Å., and Wolf-Watz, H. (1993). A secreted protein kinase of *Yersinia pseudotuberculosis* is an indispensable virulence determinant. *Nature* 361, 730–732.
- Galyov, E.E., Håkansson, S., and Wolf-Watz, H. (1994). Characterization of the operon encoding the YpkA Ser/Thr protein kinase and the YopJ protein of *Yersinia pseudotuberculosis*. *J. Bacteriol.* 176, 4543–4548.
- Grizot, S., Faure, J., Fieschi, F., Vignais, P.V., Dagher, M.C., and Pebay-Peyroula, E. (2001). Crystal structure of the Rac1-RhoGDI complex involved in nadph oxidase activation. *Biochemistry* 40, 10007–10013.
- Håkansson, S., Galyov, E.E., Rosqvist, R., and Wolf-Watz, H. (1996). The *Yersinia* YpkA Ser/Thr kinase is translocated and subsequently targeted to the inner surface of the HeLa cell plasma membrane. *Mol. Microbiol.* 20, 593–603.
- Hardt, W.D., Chen, L.M., Schuebel, K.E., Bustelo, X.R., and Galán, J.E. (1998). *S. typhimurium* encodes an activator of Rho GTPases that induces membrane ruffling and nuclear responses in host cells. *Cell* 93, 815–826.
- Henderson, D.A. (1999). The looming threat of bioterrorism. *Science* 283, 1279–1282.
- Huse, M., and Kuriyan, J. (2002). The conformational plasticity of protein kinases. *Cell* 109, 275–282.
- Inglesby, T.V., Dennis, D.T., Henderson, D.A., Bartlett, J.G., Ascher, M.S., Eitzen, E., Fine, A.D., Friedlander, A.M., Hauer, J., Koerner, J.F., et al. (2000). Plague as a biological weapon: medical and public health management. Working group on civilian biodefense. *JAMA* 283, 2281–2290.
- Juris, S.J., Rudolph, A.E., Huddler, D., Orth, K., and Dixon, J.E. (2000). A distinctive role for the *Yersinia* protein kinase: actin binding, kinase activation, and cytoskeleton disruption. *Proc. Natl. Acad. Sci. USA* 97, 9431–9436.
- Logsdon, L.K., and Mecsas, J. (2003). Requirement of the *Yersinia pseudotuberculosis* effectors YopH and YopE in colonization and persistence in intestinal and lymph tissues. *Infect. Immun.* 71, 4595–4607.
- Maesaki, R., Ihara, K., Shimizu, T., Kuroda, S., Kaibuchi, K., and Hakoshima, T. (1999a). The structural basis of Rho effector recognition revealed by the crystal structure of human RhoA complexed with the effector domain of PKN/PRK1. *Mol. Cell* 4, 793–803.
- Maesaki, R., Shimizu, T., Ihara, K., Kuroda, S., Kaibuchi, K., and Hakoshima, T. (1999b). Biochemical and crystallographic characterization of a Rho effector domain of the protein serine/threonine kinase N in a complex with RhoA. *J. Struct. Biol.* 126, 166–170.
- McCormick, J.B. (1998). Epidemiology of emerging/re-emerging antimicrobial-resistant bacterial pathogens. *Curr. Opin. Microbiol.* 1, 125–129.
- Murshudov, G.N., Vagin, A.A., and Dodson, E.J. (1997). Refinement of macromolecular structures by the maximum-likelihood method. *Acta Crystallogr. D Biol. Crystallogr.* 53, 240–255.
- Nejedlik, L., Pierfelice, T., and Geiser, J.R. (2004). Actin distribution is disrupted upon expression of *Yersinia* YopO/YpkA in yeast. *Yeast* 21, 759–768.
- Perrakis, A., Morris, R., and Lamzin, V.S. (1999). Automated protein model building combined with iterative structure refinement. *Nat. Struct. Biol.* 6, 458–463.
- Perry, R.D., and Fetherston, J.D. (1997). *Yersinia pestis*—etiologic agent of plague. *Clin. Microbiol. Rev.* 10, 35–66.
- Potterton, E., Briggs, P., Turkenburg, M., and Dodson, E. (2003). A graphical user interface to the CCP4 program suite. *Acta Crystallogr. D Biol. Crystallogr.* 59, 1131–1137.
- Rudolph, M.G., Weise, C., Mirold, S., Hillenbrand, B., Bader, B., Wittinghofer, A., and Hardt, W.D. (1999). Biochemical analysis of SopE from *Salmonella typhimurium*, a highly efficient guanosine nucleotide exchange factor for RhoGTPases. *J. Biol. Chem.* 274, 30501–30509.
- Rypniewski, W.R., Holden, H.M., and Rayment, I. (1993). Structural consequences of reductive methylation of lysine residues in hen egg white lysozyme: an X-ray analysis at 1.8-Å resolution. *Biochemistry* 32, 9851–9858.
- Scheffzek, K., Stephan, I., Jensen, O.N., Illenberger, D., and Gierschik, P. (2000). The Rac-RhoGDI complex and the structural basis for the regulation of Rho proteins by RhoGDI. *Nat. Struct. Biol.* 7, 122–126.
- Shao, F., Merritt, P.M., Bao, Z., Innes, R.W., and Dixon, J.E. (2002). A *Yersinia* effector and a *Pseudomonas* avirulence protein define a family of cysteine proteases functioning in bacterial pathogenesis. *Cell* 109, 575–588.
- Simonet, M., and Falkow, S. (1992). Invasin expression in *Yersinia pseudotuberculosis*. *Infect. Immun.* 60, 4414–4417.
- Stebbins, C.E., and Galán, J.E. (2001). Structural mimicry in bacterial virulence. *Nature* 412, 701–705.
- Terwilliger, T. (2004). SOLVE and RESOLVE: automated structure solution, density modification and model building. *J. Synchrotron Radiat.* 11, 49–52.
- Trülsch, K., Sporleder, T., Igwe, E.I., Rüssmann, H., and Heesemann, J. (2004). Contribution of the major secreted Yops of *Yersinia enterocolitica* O:8 to pathogenicity in the mouse infection model. *Infect. Immun.* 72, 5227–5234.
- Viboud, G.I., and Bliska, J.B. (2005). *Yersinia* outer proteins: role in modulation of host cell signaling responses and pathogenesis. *Annu. Rev. Microbiol.* 59, 69–89.
- Wei, Y., Zhang, Y., Derewenda, U., Liu, X., Minor, W., Nakamoto, R.K., Somlyo, A.V., Somlyo, A.P., and Derewenda, Z.S. (1997). Crystal structure of RhoA-GDP and its functional implications. *Nat. Struct. Biol.* 4, 699–703.
- Winn, M.D., Isupov, M.N., and Murshudov, G.N. (2001). Use of TLS parameters to model anisotropic displacements in macromolecular refinement. *Acta Crystallogr. D Biol. Crystallogr.* 57, 122–133.
- Winn, M.D., Murshudov, G.N., and Papiz, M.Z. (2003). Macromolecular TLS refinement in REFMAC at moderate resolutions. *Methods Enzymol.* 374, 300–321.